Effect of Laser-Induced Microstructure in Cavitation Erosion Performance of Martensitic Stainless Steel

Niroj Maharjan(✉) and Dennise Tanoko Ardi

Advanced Remanufacturing and Technology Centre, 3 CleanTech Loop, CleanTech Two, #01/01, Singapore 637143, Singapore
maharjan_niroj@artc.a-star.edu.sg

Abstract. Cavitation erosion causes material removal from the surface of metal components submerged under swift flowing fluid due to implosions of gas bubbles on their surface. Since erosion is a surface degradation phenomenon, laser surface hardening can be a promising solution to tackle this problem without affecting the bulk properties of material. Laser acts as a localized surface heater which induces rapid non-equilibrium phase transformation and produces hard microstructure near the surface. In this paper, the effect of laser-induced microstructure on cavitation erosion performance of AISI 420 martensitic stainless steel is systematically investigated. Surface hardness as high as 700 HV is recorded after laser hardening and the microstructure consisted of fine carbides and retained austenite in a martensitic matrix. Such microstructure is attributed to result in high cavitation erosion resistance. The cavitation erosion resistance of laser hardened surface was found to be 18 times higher than that of untreated surface. The results indicate the significance of microstructural transformation induced by laser treatment on erosion performance of stainless steels.

Keywords: Cavitation erosion · Laser hardening · Microstructure · Hardness · Martensitic stainless steel

1 Introduction

Machine components submerged under swiftly flowing fluid such as propellers and turbines are prone to damage by cavitation erosion [1]. The erosion occurs by sudden collapse of cavities or bubbles that form due to local fluctuation in pressure inside the fluid [2]. The damage appears as pits due to removal of material by impact of bubbles and can be quite detrimental in some cases, demonstrated by significant mass losses and rough surfaces. Generally, such erosion is prevented by using an erosion resistant material such as austenitic steel with high work hardenability [3] or improving the design of the component to reduce pressure variation [4]. However, the solution can be very costly as it involves using expensive material (like stainless steels and high speed steels) or modifying the design.

An alternative cost effective method to combat cavitation erosion is to perform surface treatment of vulnerable areas in order to increase the life of the component.

S. Itoh and S. Shukla (Eds.): INCASE 2019, LNME, pp. 321–329, 2020.
https://doi.org/10.1007/978-981-15-0054-1_34

Laser surface hardening is a well-established surface modification method which employs laser beam to increase hardness of steels [5]. It generates martensitic phase transformation near the surface due to rapid heating and cooling of the surface without affecting the bulk of the material. The method is widely used in automotive and heavy machinery industries to increase wear resistance of shafts, bearings and gears [6].

The phase transformation induced by laser treatment might have beneficial effect on improving cavitation erosion resistance. Generally, it is reported that the formation of fine-grained microstructure and increase in surface hardness produced by laser hardening contributes to significant improvement in cavitation erosion resistance [7–9]. An excellent review on cavitation erosion behavior of laser treated surfaces has been reported by Kwok et al. [10]. This indicates the potential of using laser surface treatment as a solution to tackle cavitation erosion problem. However, a systematic study investigating the influence of laser-induced microstructural changes in cavitation erosion resistance of stainless steel is still lacking.

In this study, the cavitation erosion performance of laser hardened stainless steel is investigated in detail. Cavitation tests were performed in an ultrasonic test rig which produces high frequency ultrasonic waves in a liquid to induce cavities formation near the surface of specimen. Various characterization studies such as microscopy, hardness testing and X-ray diffraction were performed to understand the effect of microstructure and properties of the hardened surface on cavitation erosion resistance. The study shows the improvement in cavitation erosion resistance after laser hardening compared to that of untreated surface.

2 Materials and Methodology

The material used for the study was AISI 420 martensitic steel, which is a corrosion resistant steel commonly used in pumps and valves that are prone to cavitation erosion. The chemical composition of the steel is shown in Table 1. Each specimen had a dimension of 40 × 40 × 10 mm^3 and was subjected to a standard stress relief heat treatment by heating in an air furnace at 650 °C for 2 h. This produced an annealed microstructure with a large number of spherical carbides randomly distributed in the matrix (see Fig. 1). The specimens were ground to an average roughness of about 0.7 μm before performing laser treatment.

Table 1. Elemental composition of AISI 420 martensitic stainless steel

Elements	C	Si	Mn	P	S	Cr	Ni	Mo	V	Cu	Al
wt%	0.41	0.33	0.74	0.025	0.001	12.69	0.16	0.05	0.046	0.05	0.017

The laser hardening trials were performed using LaserTec 65 3D system (DMG Mori) which uses a high power diode laser of 1064 nm wavelength. The laser beam was focused through a focusing lens producing a beam spot diameter of 3 mm at the specimen surface. Different operating parameters were utilized to determine the optimal parameters to achieve hardened surface without any surface melting. Based on the

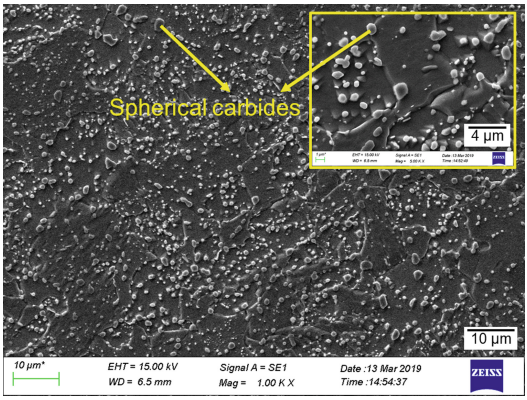

Fig. 1. A typical spheroidized microstructure of as-received steel showing carbides distributed randomly in the matrix

analysis, a laser power of 360 W and a traverse speed of 20 mm/s was chosen which delivered an energy density of about 5 J/mm^2 at the surface. The beam spot was scanned along the surface to perform a single pass laser treatment with an overlap of 60%. All the experiments were carried out in air.

For cavitation testing, an ultrasonic vibratory test setup conforming to ASTM G32-16 standard was utilized. Both as-received as well as laser hardened specimens were tested for comparison. The specimen was held stationary below the vibrating horn at a distance of 0.5 mm. The vibration frequency and peak-to-peak amplitude were 20 kHz and 50 µm respectively. The testing was performed for a total of 15 h with mass loss recorded at 1 h interval. The cavitation medium was distilled water maintained at a constant room temperature of 25 ± 2°C.

The laser hardened surface and the eroded surface were characterized using optical microscope (Zeiss Axioscope A1) and electron microscope (Zeiss Evo HD25). Standard metallographic technique was implemented to study the cross-section microstructure of laser-hardened surface. Hardness measurements were performed using Vickers hardness indenter at 100 gf with 15 s dwell time. Furthermore, X-ray diffraction data were collected using Panalytical Empyrean X-ray diffractometer. The diffractometer used a copper target as a source of X-ray with wavelength λ = 1.5404 Å (Cu $K_{\alpha 1}$). The residual stresses along the depth were measured by electrospeckle pattern interferometry (ESPI) with hole drilling method (StressTech PRISM).

3 Results and Discussion

3.1 Characterization of Laser Hardened Surface

Figure 2 shows a typical cross-microstructure of the steel near the surface after laser hardening. The microstructure is clearly distinct from the parent microstructure. It consisted of refined microstructure with numerous δ-ferrite dendrites in martensitic matrix and some retained austenite. The rapid heating by the laser energy results in rapid

austenitization of the surface and produces non-equilibrium microstructure due to rapid cooling as the heat is conducted to the bulk of the material [11]. An affected region of about 660 μm thickness formed with the laser parameter chosen. The microstructure varied gradually along the depth due to decreasing influence of laser heating.

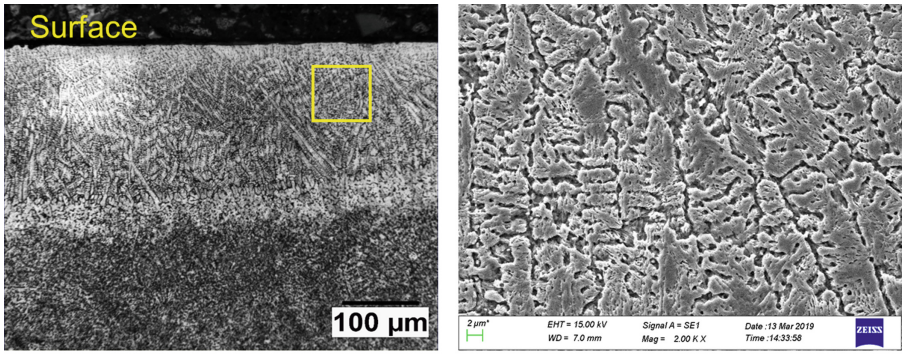

Fig. 2. Cross section microstructure of laser hardened steel showing (a) laser hardened region near the surface, and (b) magnified image of square inset in (a)

X-ray diffraction data was collected to verify the phases formed after laser hardening. Figure 3 compares the XRD diffractograms of as-received and laser hardened specimens. As observed in the micrographs, the as-received specimen consisted of ferrite peaks and laser hardened surface revealed peaks of martensite, austenite, carbides and some oxides.

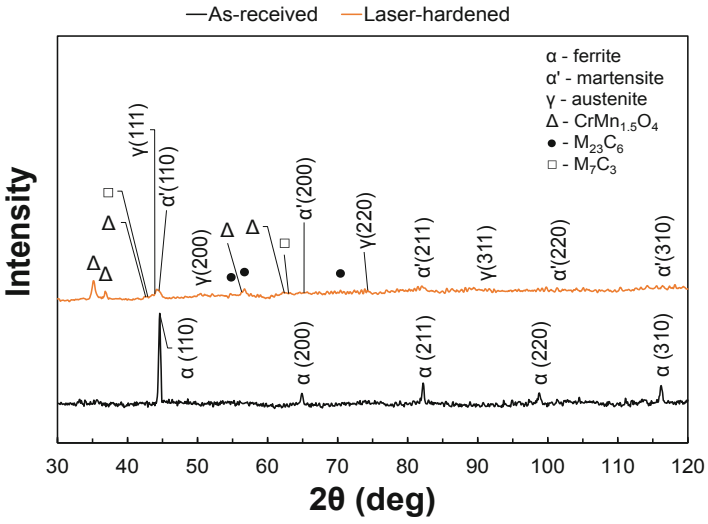

Fig. 3. X-ray diffraction data of as-received and laser hardened surfaces

The hardness measurements also supported the microstructure and phases observed from microscopy and XRD. As seen in Fig. 4, the laser hardened surface had a very high hardness (∼700 HV) owing to the presence of hard martensite and microstructure refinement. The hardness decreased gradually along the depth. This suggests the decreasing volume fraction of martensite along the depth due to decreasing effect of laser heating [12]. The values reach the base material hardness at about 700 μm which matches with the laser-affected region measured by optical microscopy.

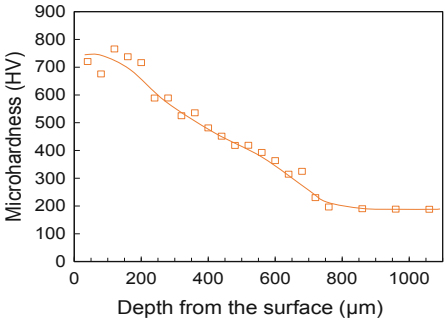

Fig. 4. Variation of microhardness along the depth for laser hardened specimen

Furthermore, the residual stresses induced by laser hardening is shown in Fig. 5. The as-received surface had slightly tensile residual stresses near the surface due to prior machining and polishing of the surface. In case of laser hardened specimen, compressive residual stresses were found near the surface which reached its maximum value of ∼ −300 MPa at the depth of about 180 μm. At higher depths, the stress state changed to tensile and reached very high tensile stresses at around 680 μm. The residual stresses in laser hardened components arise from combination of volumetric dilatation due to phase transformation and thermal residual stresses [13]. Near the surface, the volume expansion due to martensitic phase transformation suppresses tensile thermal stresses and thus, produces net beneficial compressive residual stresses. At higher depths, however, the thermal effect is dominant and thus results in tensile stresses.

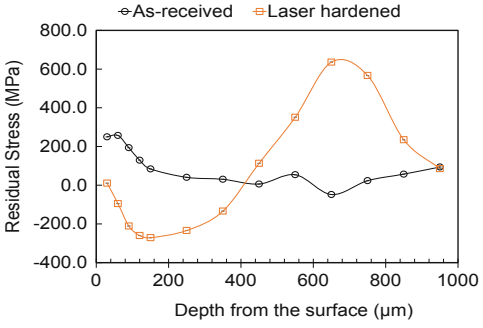

Fig. 5. Distribution of residual stresses along the depth for both as-received and laser hardened specimen

3.2 Cavitation Erosion Performance

The cumulative mass loss during cavitation test of the specimens tested as a function of time are plotted in Fig. 6. The as-received specimen did not show any appreciable mass loss up to 3 h of testing, which suggests the erosion is still in incubation phase. After 3 h, the mass loss increases linearly and reached up to 70 mg after 15 h of testing.

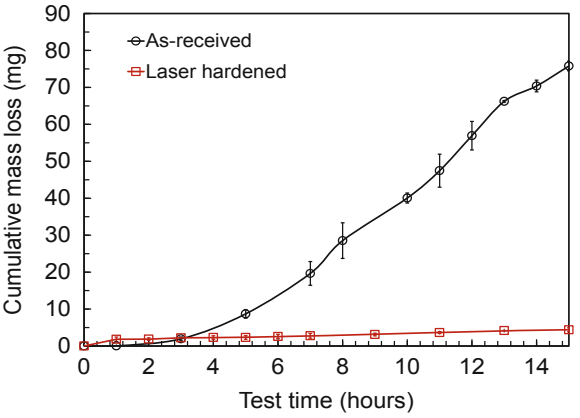

Fig. 6. Graph showing cumulative mass loss of the steel specimen against time during cavitation erosion test

Compared to as-received specimen, laser hardened specimen exhibited very little mass loss. Interestingly, a careful observation of the mass loss at initial stage shows the mass loss starts as early as 1 h of testing for laser hardened specimen. This is probably due to the removal of oxide layers from the surface which formed during laser hardening in air [14]. Nevertheless, the cumulative mass loss still does not increase tremendously as compared to as-received specimen. A mere mass loss of about 9.5 mg was recorded even after 40 h of testing.

Table 2 summarizes the cavitation performance of as-received and laser hardened surfaces after 15 h of testing. It can be seen that the cavitation erosion resistance of laser hardened specimen is about 18 times higher than that of as-received specimen. This shows that laser hardening enhances cavitation erosion resistance of 420 martensitic stainless steel.

Table 2. Comparison of cavitation erosion performance of as-received and laser hardened surfaces after 15 h of cavitation erosion testing

Specimen	Cumulative mass loss (mg)	Mean depth of erosion (μm)	Mean erosion rate (μm/h)	Cavitation erosion resistance (Re) (h/μm)
As-received	75.79	5.73	5.73	0.17
Laser hardened	4.39	0.65	0.33	3.06

Figure 7(a) shows the morphology of eroded surface after 15 h of cavitation testing. Due to extensive plastic deformation, the as-received specimens exhibited deep craters on the surface. The damage occurred due to localized pile up of plastic deformation by impact of micro-jets generated from sudden collapse of cavities [15]. Some work hardening might have occurred on the surface which after exceeding the strength of the material results in nucleation of cracks. The cracks then quickly propagate and co-lease producing brittle surface fracture. The phenomenon is repeated at multiple regions by collapsing of bubbles which finally manifests as pits and severe surface undulations. The damage on the laser hardened surface was superficial and less severe as shown in Fig. 7(b). A closer observation of the specimen showed early stage of cavitation with lots of shallow craters on the surface. This suggests the resistance of the hardened surface prevented formation of deep pits.

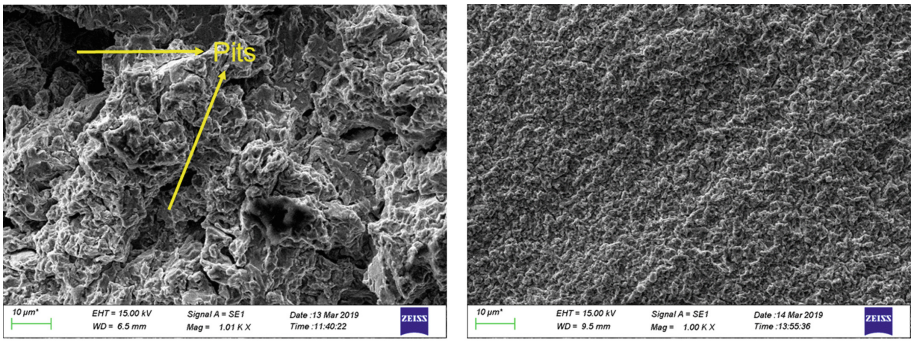

Fig. 7. Surface morphology after 15 h of cavitation erosion testing for (a) as-received surface, and (b) laser hardened surface

The higher cavitation resistance of laser hardened specimen reveals the significance of microstructure evolution in improving cavitation performance. Laser hardening produced martensitic phase transformation. Martensite is considered beneficial as it provides a cushioning effect during collapsing of bubbles by taking up some of the impact energy [16, 17]. In addition, it increases surface hardness which is often attributed to increase in cavitation erosion resistance [18, 19]. Moreover, the presence of retained austenite improves toughness of the material [20]. Furthermore, the compressive stresses are known to attenuate the crack initiation and propagation during loading. However, the influence of residual stresses is difficult to judge from the results as it had very little compressive residual stresses near the surface. Therefore, the results indicate the proper combination of martensite and retained austenite formed by laser hardening has beneficial effect on improving cavitation erosion resistance of AISI 420 martensitic stainless steel.

4 Conclusions

In this study, laser hardening of AISI 420 stainless steel was performed to investigate its effect on cavitation erosion performance and the results are compared with that of untreated steel. It was found that the cavitation erosion resistance of laser hardened steel is ~18 times higher than untreated steel after 15 h of cavitation erosion testing. Such improvement in cavitation erosion resistance is attributed to rapid non-equilibrium phase transformation produced by laser induced hardening. The fast heating and cooling by laser beam produces a refined microstructure consisting of martensite, retained austenite and carbides. The surface microstructure resists cavitation damage by virtue of its high hardness and resilience to fracture. Further work is being done to control the microstructure evolution during laser hardening using different processing parameters and evaluate its effect on cavitation erosion resistance.

Acknowledgements. Support for this work was provided by A*STAR Advanced Remanufacturing and Technology Centre (ARTC), Singapore under the In-house Research Project ARTC19_01_DSE. The authors thank Prof. Yeo Swee Hock at Nanyang Technological University, Singapore for assisting in cavitation test rig setup and Mr. Lek Yung Zhen for his help in performing cavitation erosion tests.

References

1. Karimi, A., Martin, J.L.: Cavitation erosion of materials. Int. Met. Rev. **31**, 1–26 (1986)
2. Sreedhar, B.K., Albert, S.K., Pandit, A.B.: Cavitation damage: theory and measurements–a review. Wear **372**, 177–196 (2017)
3. Liu, W., Zheng, Y.G., Liu, C.S., et al.: Cavitation erosion behavior of Cr–Mn–N stainless steels in comparison with 0Cr13Ni5Mo stainless steel. Wear **254**, 713–722 (2003)
4. Schiavello, B., Visser, F.C.: Pump Cavitation: various NPSHR criteria, NPSHA margins, impeller life expectancy. In: Proceedings of the 25th International Pump Users Symposium. Texas A&M University. Turbomachinery Laboratories (2009)
5. Maharjan, N.: Laser surface hardening of bearing steels (2019)
6. Nath, A.K., Sarkar, S.: Laser transformation hardening of steel. In: Advances in Laser Materials Processing, pp. 257–298. Elsevier (2018)
7. Kwok, C.T., Man, H.C., Cheng, F.T.: Cavitation erosion and pitting corrosion behaviour of laser surface-melted martensitic stainless steel UNS S42000. Surf. Coat. Technol. **126**, 238–255 (2000)
8. Lo, K.H., Cheng, F.T., Man, H.C.: Laser transformation hardening of AISI 440C martensitic stainless steel for higher cavitation erosion resistance. Surf. Coat. Technol. **173**, 96–104 (2003)
9. Mann, B.S.: Water droplet erosion behavior of high-power diode laser treated 17Cr4Ni PH stainless steel. J. Mater. Eng. Perform. **23**, 1861–1869 (2014)
10. Kwok, C.T., Man, H.C., Cheng, F.T., Lo, K.H.: Developments in laser-based surface engineering processes: with particular reference to protection against cavitation erosion. Surf. Coat. Technol. **291**, 189–204 (2016)
11. Ashby, M.F., Easterling, K.E.: The transformation hardening of steel surfaces by laser beams —I. Hypo-eutectoid steels. Acta Metall. **32**, 1935–1948 (1984)

12. Bojinović, M., Mole, N., Štok, B.: A computer simulation study of the effects of temperature change rate on austenite kinetics in laser hardening. Surf. Coat. Technol. **273**, 60–76 (2015). https://doi.org/10.1016/j.surfcoat.2015.01.075
13. Bailey, N.S., Tan, W., Shin, Y.C.: Predictive modeling and experimental results for residual stresses in laser hardening of AISI 4140 steel by a high power diode laser. Surf. Coat. Technol. **203**, 2003–2012 (2009)
14. Maharjan, N., Zhou, W., Zhou, Y., Wu, N.: Influence of operating parameters on morphology of laser hardened surfaces. In: High-Power Laser Materials Processing: Applications, Diagnostics, and Systems VII. International Society for Optics and Photonics (2018)
15. Dular, M., Požar, T., Zevnik, J.: High speed observation of damage created by a collapse of a single cavitation bubble. Wear **418**, 13–23 (2019)
16. Park, M.C., Shin, G.S., Yun, J.Y., et al.: Damage mechanism of cavitation erosion in austenite → martensite phase transformable Fe–Cr–C–Mn/Ni alloys. Wear **310**, 27–32 (2014)
17. Wang, K.Y., Lo, K.H., Kwok, C.T., et al.: The influences of martensitic transformations on cavitation-erosion damage initiation and pitting resistance of a lean austenitic stainless steel. Mater. Res. **19**, 1366–1371 (2016)
18. Espitia, L.A., Dong, H., Li, X.-Y., et al.: Cavitation erosion resistance and wear mechanisms of active screen low temperature plasma nitrided AISI 410 martensitic stainless steel. Wear **332**, 1070–1079 (2015)
19. da Severo, F.S., Scheuer, C.J., Cardoso, R.P., Brunatto, S.F.: Cavitation erosion resistance enhancement of martensitic stainless steel via low-temperature plasma carburizing. Wear **428**, 162–166 (2019)
20. Wu, R., Li, W., Zhou, S., et al.: Effect of retained austenite on the fracture toughness of quenching and partitioning (Q&P)-treated sheet steels. Metall. Mater. Trans. A **45**, 1892–1902 (2014)